24th INTERNATIONAL CONGRESS ON SOUND AND VIBRATION
23–27 July 2017, London

ICSV24
23-27JULY 2017
LONDON CALLING

ADAPTIVE ACOUSTIC METASURFACES FOR THE NOISE SHIELDING

Pavel Mokrý, Jan Václavík, Jakub Nečásek
Technical University of Liberec, Faculty of Mechatronics, Informatics and Interdisciplinary Studies, Studentská 2, liberec, Czech Republic
email: pavel.mokry@tul.cz

Pavel Psota, Kateřina Steiger, David Vápenka
Institute of Plasma Physics of the Czech Academy of Sciences, Regional Center for Special Optics and Optoelectronic Systems (TOPTEC), Za Slovankou 1782/3, Prague, Czech Republic

It is known that active acoustic metasurfaces (AAMSs), which consist of the curved glass shell with attached piezoelectric transducers, can provide efficient means for the noise shielding. The principle standing behind this effect is based on the electronic control of the acoustic impedance (AI) of the AAMS, which is achieved by connecting the piezoelectric transducers to the active shunt circuits. When the connected shunt circuit has a required value of the complex electrical impedance, it is possible to achieve extremely high negative values of the AI of the AAMS. This regime is often called the negative elasticity regime (NER) of the AAMS. In the NER, the incident sound wave can be completely reflected and the transmitted sound vanishes. Unfortunately, the working point of the electrical circuit is located near the edge of the stability region, when the AMMS operates in the NER. In this Paper, we demonstrate experimentally that it is possible to construct an adaptive AMMS, which is stable in varying operational conditions. The adaptive AMMS is achieved by introducing an additional feedback loop for the control of the required value of the AI. This is attained by introducing the system for the real-time estimation of the AI value and the accurate control of the complex electrical impedance of the shunt circuit by means of the iterative algorithm.

Keywords: acoustic metasurface, noise shielding, piezoelectric actuators, negative elasticity

1. Introduction

It is known that the increase in the acoustical transmission loss of sound passing through the planar structures represents a quite challenging research task in the field of noise control [1]. The reason for the low noise shielding efficiency of large planar structures is the low flexural rigidity. A very efficient mean for increasing the acoustic transmission loss of plates and shells is offered by the use of piezoelectric actuators, which are connected to passive or active electrical networks [2, 3]. It was shown by Date [4] that the macroscopic Young's modulus of piezoelectric transducers can be controlled to a large extent by connecting them to the active shunt circuits, which have negative capacitance (NC). This approach has been afterwards referred as the Active Elasticity Control (AEC).

The AEC method allowed the construction of noise isolation devices, which were based on the use of thin piezoelectric membranes [5, 6]. Fukada et al. [7] have discovered that the thin piezoelectric polymer film shunted by NC circuit can enter the negative elasticity regime (NER). Thus, the piezoelectric polymer films shunted with NC circuits posses the features, which are nowadays attributed to

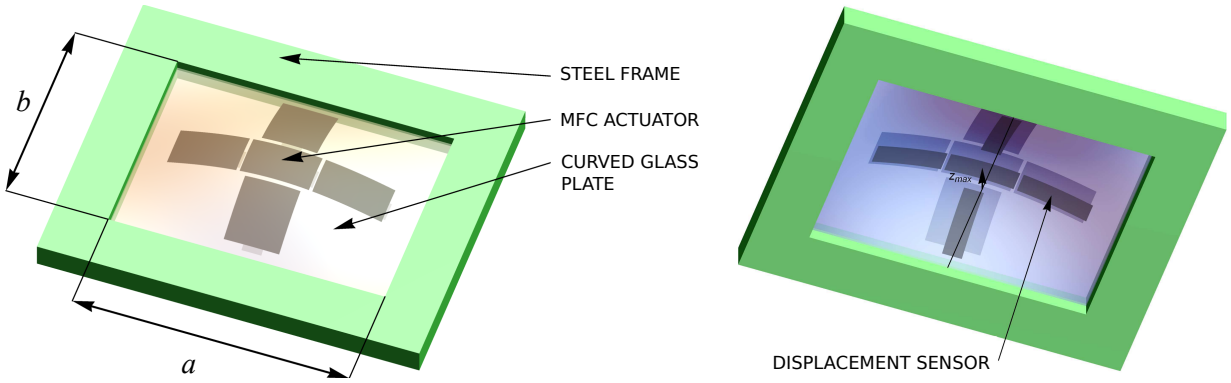

(a) Top view (b) Bottom view

Figure 1: Top (a) and bottom (b) views of the constructed adaptive acoustic metasurface. It consists of the curved glass plate fixed in a rigid steel frame. The macro fiber composite (MFC) piezoelectric actuators and sensors are attached on the top and bottom surfaces of the glass shell, respectively.

active acoustic metamaterials [8] and metasurfaces [9]. The greatest advantage of the AEC is the fact that the negative values of elastic properties do not require any particular resonance behaviour in any sub-wavelength periodic structure. The NER is achieved by the action of the electronic shunt circuit, and, thus, it can be produced in the arbitrary frequency frequency range.

Despite clear advantages, the greatest drawback of the AEC is a sensitivity to the adjustment of the shunt circuit. This drawback makes it difficult to achieve the required values of the acoustic transmission loss in varying operating conditions. It was demonstrated by Sluka et al. [10, 11] and by Kodejška et al. [12] that this drawback can be eliminated in simple one-dimensional acoustic systems by means of an iterative adaptive algorithm for automatic adjustment of the NC circuit.

The aforementioned issues have motivated the work presented below, where we addressed the problem of self-adjustment of the noise isolation system, which consists of the active acoustic metasurface with large areal dimensions.

2. Noise shielding by means of active acoustic metasurfaces

Figure 1 shows the constructed adaptive acoustic metasurface (AAMS). It consists of the curved glass plate fixed in a rigid steel frame. The macro fiber composite (MFC) piezoelectric actuators and sensors are attached on the top and bottom surfaces of the glass shell, respectively. The dimensions of the curved glass plate are $a = 0.42$ m and $b = 0.3$ m. Thicknesses of the glass plate and of the MFC actuators are $h_g = 5$ mm and $h_{\mathrm{MFC}} = 0.3$ mm, respectively. The profile of the curved glass plate is given by the function $z_{max} \sin(\pi x/a) \sin(\pi y/b)$, where $z_{max} = 5$ mm.

The propagation of acoustic energy associated with the transmission of noise through planar interfaces is controlled by a physical property called specific acoustic impedance z_m. In the case of planar interface, the value of specific acoustic impedance (in Pa s m^{-1}) is defined as a ratio of acoustic sound pressure p over the particle velocity v:

$$z_m = p/v. \tag{1}$$

The efficiency of the sound shielding is frequently expressed using the physical quantity called acoustic transmission loss $\mathtt{TL}$, which can be expressed in terms of z_m:

$$\mathtt{TL} = 20 \log_{10} \left| 1 + \frac{z_m}{2 z_a} \right|, \tag{2}$$

where $z_a = \varrho_0 c$ is the characteristic acoustic impedance of air, ϱ_0 is the air density and c is the sound velocity in the air. In the frequency range around the first resonance mode of the curved glass shell

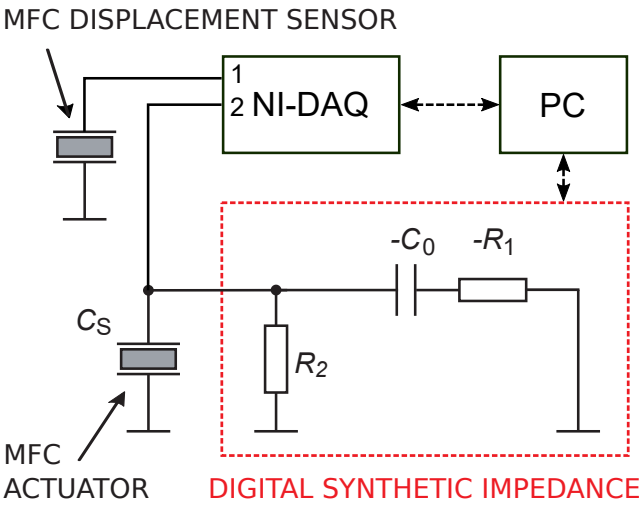

Figure 2: Electrical scheme of the adaptive acoustic metasurface (AAMS).

and considering $a > b \gg h_g > h_{\mathrm{MFC}}$, the specific acoustic impedance z_m of the considered noise shielding plate can be approximated by the formula [13]:

$$z_m(\omega) \approx \frac{i\pi^2 \left(h_g + h_{\mathrm{MFC}}\right)}{16\,\omega} \left[\varrho\omega^2 - \xi Y \left(1 + \frac{i}{Q_m}\right)\right], \tag{3}$$

where $\xi = \left(2\nu\xi_x\xi_y + \xi_x^2 + \xi_y^2\right) / \left(1 - \nu^2\right)$ is the average inverse radius of curvature of the shell, ξ_x and ξ_y stand for the average inverse radii of curvature of the glass shell along the x and y coordinates,

$$Y = \frac{Y_g h_g + Y_{\mathrm{MFC}} h_{\mathrm{MFC}}}{h_g + h_{\mathrm{MFC}}} \tag{4}$$

is the macroscopic Young's modulus of the composite structure. Symbols ν, ρ, and Q_m are the average Poisson ratio, mass density, and mechanical quality factor of the AAMS. Symbols Y_g and Y_{MFC} stand for the Young's modulus of the glass plate and for the piezoelectric MFC actuator. Symbol ω is the angular frequency of the incident sound wave, and $i = \sqrt{-1}$.

The principal result of the AEC method developed by Date et al. [4] is the effective dynamic value of the Young's modulus of the piezoelectric transducer, which is shunted by the external capacitance C:

$$Y_{\mathrm{MFC}} = Y_S \left(\frac{1 + \alpha}{1 - k^2 + \alpha}\right), \tag{5}$$

where k^2 is the electromechanical coupling factor, C_S is the capacitance of the piezoelectric transducer, and $\alpha = C/C_S$. It follows from Eq. (5) that, when

$$C \to -(1 - k^2)\, C_S, \tag{6}$$

the macroscopic value of Young's modulus reaches large values.

Figure 2 shows the electrical scheme of the AAMS. The piezoelectric transducer of capacitance C_S is shunted by the digital synthetic impedance (DSI), which implements the NC circuit [14]. In our particular experiment, the DSI emulates the electrical response of the RC network with the equivalent circuit shown in the red dashed area in Fig. 2. The RC network consists of the resistor R_2 connected in parallel with the in-series connection of the capacitor $-C_0$ and the resistor $-R_1$. The minuses indicate that the effective values of particular emulated electrical components are negative. The voltage applied to the MFC actuator from the DSI and the signal from the displacement sensor are fed into the data acquisition device (NI-DAQ). The acquired signals are processed by the personal computer (PC), which adjusts the effective electrical parameters $-C_0$, $-R_1$, and R_2 of the equivalent electrical circuit emulated by the DSI.

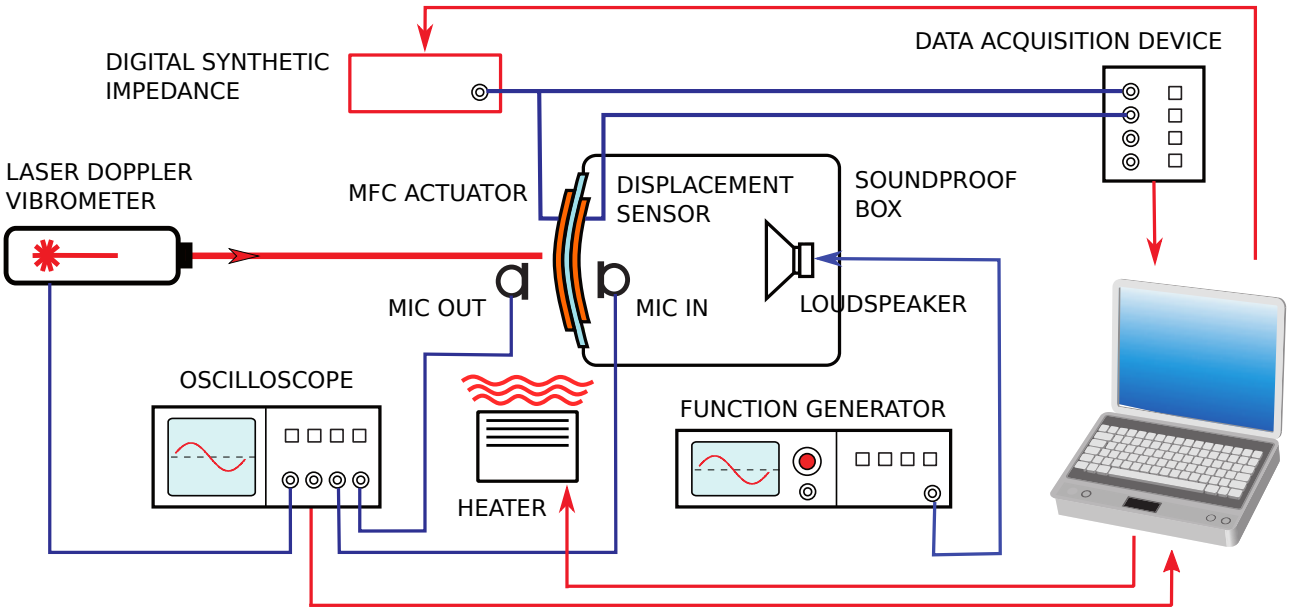

Figure 3: Scheme of the measurement of the acoustic transmission loss of the AAMS.

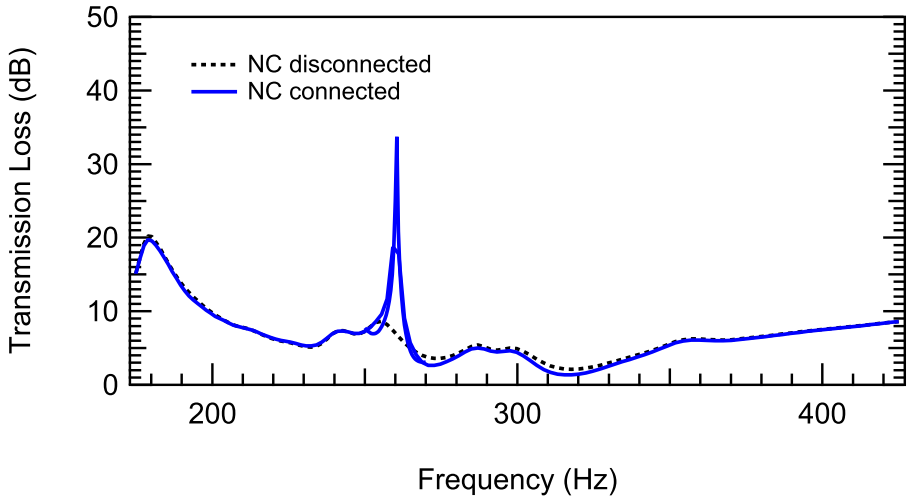

Figure 4: Frequency dependence of the acoustic transmission loss of sound transmitted through the AAMS shown in Fig. 1.

3. Results of acoustic measurements

Figure 3 shows the scheme of the experimental setup for the measurement of the noise isolation efficiency of the AAMS. The AAMS forms a lid of the soundproof box with a loudspeaker. The microphone IN, inside the soundproof box, and the microphone OUT, outside the soundproof box, measure the difference of acoustic pressures Δp at the opposite sides of the AAMS. A laser Doppler vibrometer measures the amplitude of the vibration velocity v of the middle point of the glass plate. The specific acoustic impedance z_m is approximated by the ratio $\Delta p/v$, and the value of the acoustic TL is estimated using Eq. (2). The MFC piezoelectric actuators on the AAMS are connected to the DSI. The voltage applied to the MFC actuator and the signal from the displacement sensor are fed into the data acquisition device. The iterative algorithm based on the works by Sluka et al. [11] and Kodejska et al. [12] is implemented in the PC, which controls the effective electrical parameters of the equivalent circuit emulated by the DSI. The change in the operating temperature of the AAMS is achieved by the heater.

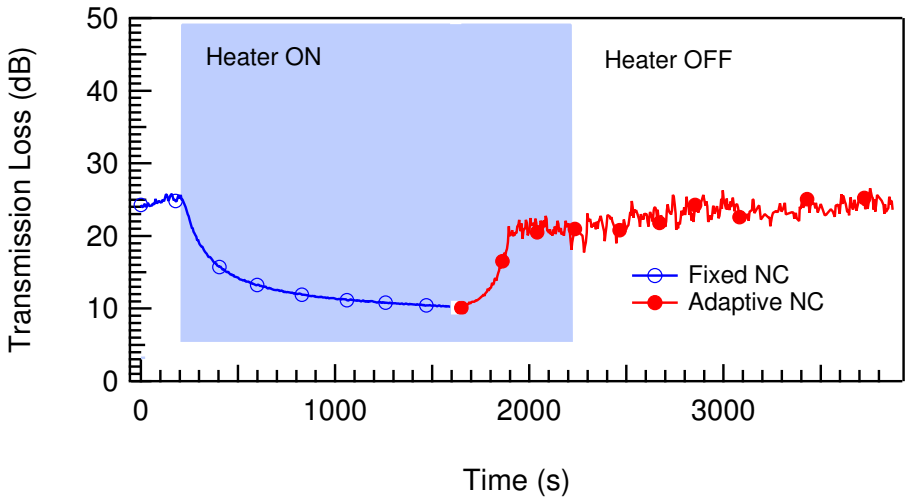

Figure 5: The time dependence acoustic transmission loss of sound of the harmonic time dependence of the frequency 260 Hz in the fixed a adaptive regimes of the AAMS.

Figure 4 shows the frequency dependence of the acoustic transmission loss of sound transmitted through the AAMS shown in Fig. 1. The dotted line shows the TL in the situation, when the DSI emulating the NC circuit is disconnected from the MFC piezoelectric actuators in the AAMS. The solid line shows the frequency dependence of TL, when the DSI is connected to the MFC piezoelectric actuators in the AAMS and the electrical parameters $-C_0$, $-R_1$, and R_2 are adjusted in such a way that the condition given by Eq. (6) is satisfied at the frequency 260 Hz. The increase in the value of Y_{MFC} due to the action of the shunt DSI yielded the increase in the value of TL through the AAMS by about 25 dB.

Figure 5 shows the principal result of this work, i.e. the time dependence of the acoustic transmission loss of pure tone sound of the frequency 260 Hz in the fixed a adaptive regimes of the constructed AAMS. The line with open markers indicate values of TL of the AAMS with a fixed adjustment of the DSI, which was adjusted at the beginning of our experiment to achieve the 25 dB acoustic transmission loss of a pure tone sound at the frequency 260 Hz. At the time 200 s the heater in the vicinity of the AAMS was turned on. The gradual change in the ambient temperature yielded the change in the value of C_S due to the pronounced temperature dependence of permittivity of ferroelectric ceramics in the MFC actuator. The fixed value of C yielded the gradual failure of the condition expressed by Eq. (6). After 1300 s, the change in the ambient temperature and the change in the value of C_S yielded the decrease in the TL through the AAMS by more than 15 dB. At the time 1600 s, the self-adjustment iterative algorithm was activated in the PC. The AAMS recovered its TL value, which is indicated by the line with filled markers. At the time 2200 s, the heater was turned off and the ambient temperature gradually decreased. The iterative algorithm implemented in the PC has, however, applied corrections to the adjustment of the effective electrical parameters of the equivalent shunt circuit emulated by the DSI, so that the condition expressed by Eq. (6) was satisfied with a high accuracy.

Figure 6 shows the frequency dependence of the acoustic transmission loss of sound transmitted through the adaptive acoustic metasurface at several stages of the acoustic experiment presented in Fig. 5. The dotted line shows the frequency dependence of TL, when the DSI was disconnected from the MFC actuators of the AAMS. The dashed line shows the frequency dependence of the TL, when the NC circuit was initially adjusted. The dashed-and-dotted line shows the frequency dependence of the TL of sound transmitted through the AAMS with the fixed initial adjustment, when the ambient temperature was changed. It indicates that the noise shielding effect of the AAMS greatly deteriorated. This represents the main drawback of the classical AEC method with the fixed adjustment of the DSI. The solid line indicates the frequency dependence of the AAMS in a situation, when the adaptive iterative algorithm applied changes to the adjustment of the effective parameters of

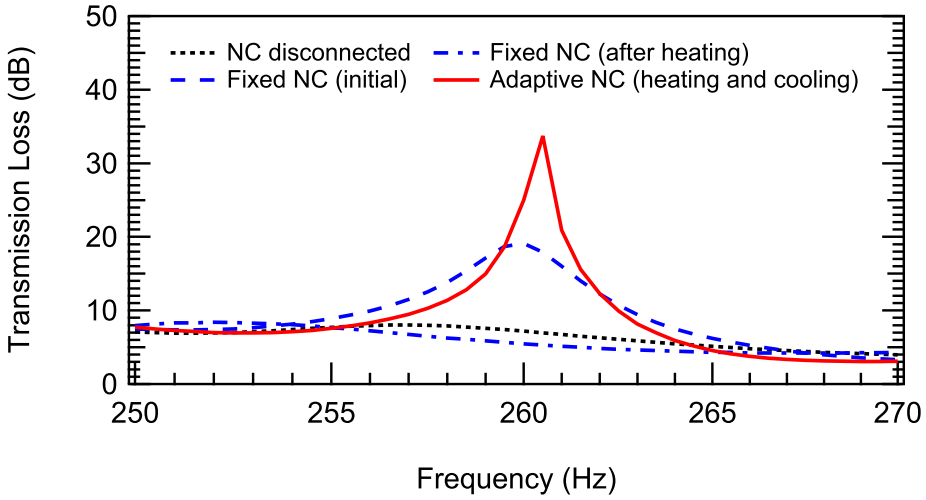

Figure 6: Frequency dependence of the acoustic transmission loss of sound transmitted through the adaptive acoustic metasurface at several stages of the acoustic experiment presented in Fig. 5

the equivalent electrical circuit emulated by the DSI.

Figure 7 demonstrates the operation of the AAMS. The color of the contour plot indicates the absolute value of the particle velocity near the AAMS as a function of the effective parameters $-C_0$ and $-R_1$ of the equivalent electrical circuit, which is emulated by the DSI. Blue and red color correspond to minimal and maximal values of the absolute particle velocity in arbitrary units, respectively. The graph corresponds to the situation of the elevated temperature at the time 1600 s in Fig. 5. Dashed lines correspond to values of the phase difference of the signals measured by the NI-DAQ. The yellow and brown points indicate the values of the adjustments of the electrical parameters $-C_0$ and $-R_1$ of the equivalent electrical circuit emulated by the DSI in the AAMS during the self-adjustment iterative process. The criterion for the corrections to the emulated effective values $-C_0$ and $-R_1$ is computed using the iterative algorithm [12, 15], which uses the values of the phase difference of the signals measured by the NI-DAQ and visualized by the dashed lines.

4. Conclusions

We analyzed the possibility of increasing the acoustic transmission loss of sound transmitted through the AAMS. A promising approach for the suppression of noise transmission through glass plates and shells using piezoelectric MFC actuators and negative capacitance circuits has been presented. Using active shunt circuits with a negative capacitance, the effective elastic properties of the piezoelectric layers can be controlled to a large extent in accordance with the principles of the AEC method. As a result, an appreciable increase in the acoustic transmission loss through the AAMS can be achieved.

The essential drawback of the conventional AEC method is a high sensitivity to the operating conditions. The deteriorating effect of the varying ambient temperature on the value of the acoustic transmission loss of the AAMS has been demonstrated by inserting the heater in the experimental measurement system. Due to the change in the operating temperature of the AAMS, the value of acoustic transmission loss has decreased by more than 15 dB. In order to eliminate the deteriorating effect of temperature change on the value of $\mathtt{TL}$, the iterative control algorithm for automatic adjustment of the electrical parameters $-C_0$ and $-R_1$ of the equivalent electrical circuit emulated by the DSI was implemented.

The implemented iterative control algorithm is based on the iterative control law developed by Sluka et al. [11] and Kodejska et al. [12]. The adopted principles of the iterative control law have been further developed and generalized, so that they become applicable to 2D large planar AAMS

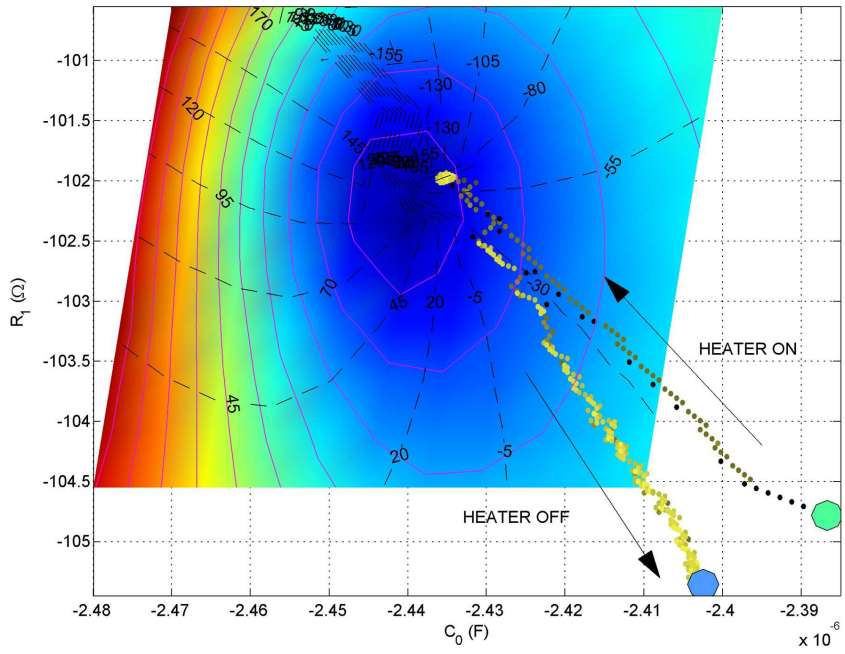

Figure 7: Demonstration of the operation of the adaptive acoustic metasurface. The color of the contour plot indicates the absolute value of the particle velocity near the adaptive acoustic metasurface. Blue and red color correspond to minimal and maximal values in arbitrary units, respectively. Dashed lines correspond to values of the phase difference of the signals measured by the NI-DAQ. The plotted points indicate the values of the adjustments of the electrical parameters $-C_0$ and $-R_1$ of the equivalent electrical circuit emulated by the DSI in the AAMS.

system. In order to make the AAMS working in varying operating condition, several additional technical difficulties had to be solved.

All in all, we believe that this method represents an important alternative technique in the field of noise control and offers several advantages (e.g., suppression of noise transmission at high frequencies with significantly smaller control rate compared with the classic ANC method) that will be ready to be applied in all contemporary applications where the classic methods are already in use (e.g., airspace industry and airplane cockpits). It also offers cheap, simple, and low-weight noise suppression devices that can be profitably used in airplanes, high-speed trains, and other noisy environments.

Acknowledgements

This work was supported by Czech Science Foundation Project No.: 16-11965S, co-financed from Ministry of Education, Youth and Sports of the Czech Republic in the Project No. NPU LO1206. Authors would like to thank Zbyněk Koldovský for reading the manuscript.

References

1. Moheimani, S. O. R. and Fleming, A. J., *Piezoelectric transducers for vibration control and damping*, Springer, London (2006).

2. Forward, R. L. Electronic damping of vibrations in optical structures, *Applied Optics*, **18** (5), 690, (1979).

3. Hagood, N. W. and von Flotow, A. Damping of structural vibrations with piezoelectric materials and passive electrical networks, *Journal of Sound and Vibration*, **146**, 243–268, (1991).

4. Date, M., Kutani, M. and Sakai, S. Electrically controlled elasticity utilizing piezoelectric coupling, *Journal of Applied Physics*, **87** (2), 863–868, (2000).

5. Mokry, P., Fukada, E. and Yamamoto, K. Noise shielding system utilizing a thin piezoelectric membrane and elasticity control, *Journal of Applied Physics*, **94** (1), 789–796, (2003).

6. Mokry, P., Fukada, E. and Yamamoto, K. Sound absorbing system as an application of the active elasticity control technique, *Journal of Applied Physics*, **94** (11), 7356–7362, (2003).

7. Fukada, E., Date, M., Kodama, H. and Oikawa, Y. Elasticity control of curved piezoelectric polymer films, *Ferroelectrics*, **320** (1), 471–481, (2005).

8. Popa, B.-I., Zigoneanu, L. and Cummer, S. A. Tunable active acoustic metamaterials, *Physical Review B*, **88** (2), 024303, wOS:000321856400002, (2013).

9. Xie, Y., Wang, W., Chen, H., Konneker, A., Popa, B.-I. and Cummer, S. A. Wavefront modulation and subwavelength diffractive acoustics with an acoustic metasurface, *Nature Communications*, **5**, 5553, wOS:000345913600017, (2014).

10. Sluka, T. and Mokrý, P. Feedback control of piezoelectric actuator elastic properties in a vibration isolation system, *Ferroelectrics*, **351**, 51–61, 8th European Conference on Applications of Polar Dielectrics (ECAPD-8), Metz, FRANCE, SEP 05-08, 2006, (2007).

11. Sluka, T., Kodama, H., Fukada, E. and Mokrý, P. Sound shielding by a piezoelectric membrane and a negative capacitor with feedback control, *IEEE Transactions on Ultrasonics, Ferroelectrics, and Frequency Control*, **55** (8), 1859–1866, (2008).

12. Kodejska, M., Mokry, P., Linhart, V., Vaclavik, J. and Sluka, T. Adaptive vibration suppression system: an iterative control law for a piezoelectric actuator shunted by a negative capacitor, *IEEE Transactions on Ultrasonics Ferroelectrics and Frequency Control*, **59** (12), 2785–2796, (2012).

13. Novakova, K., Mokry, P. and Vaclavík, J. Application of piezoelectric macro-fiber-composite actuators to the suppression of noise transmission through curved glass plates, *IEEE Transactions on Ultrasonics, Ferroelectrics and Frequency Control*, **59** (9), 2004–2014, (2012).

14. Nečásek, J., Václavík, J. and Marton, P. Digital synthetic impedance for application in vibration damping, *Review of Scientific Instruments*, **87** (2), 024704, (2016).

15. Steiger, K., Mokrý, P., Václavík, J., Psota, P., Doleček, R., Vápenka, D., Nečásek, J. and Koldovský, Z. Adaptive acoustic metasurfaces for the active sound field control, *Proceedings of the 22nd International Congress on Acoustics*, Buenos Aires, Sep., pp. ICA2016–597, Asociación de Acústicos Argentinos, (2016).